THERMAL BEHAVIOR IN THE LENS PROCESS

M. L. Griffith, M. E. Schlienger,
L. D. Harwell, M. S. Oliver, M. D. Baldwin, M. T. Ensz,
J. E. Smugeresky*, M. Essien, J. Brooks, and C. V. Robino
Sandia National Laboratories[#], Albuquerque, NM, *Livermore, CA

W. H. Hofmeister and M. J. Wert
Vanderbilt University, Memphis, TN

D. V. Nelson
Stanford University, Stanford, CA

Introduction

Direct laser metal deposition processing is a promising manufacturing technology which could significantly impact the length of time between initial concept and finished part. For adoption of this technology in the manufacturing environment, further understanding is required to ensure robust components with appropriate properties are routinely fabricated. This requires a complete understanding of the thermal history during part fabrication and control of this behavior. This paper will describe our research to understand the thermal behavior for the Laser Engineered Net Shaping (LENS) process[1], where a component is fabricated by focusing a laser beam onto a substrate to create a molten pool in which powder particles are simultaneously injected to build each layer. The substrate is moved beneath the laser beam to deposit a thin cross section, thereby creating the desired geometry for each layer. After deposition of each layer, the powder delivery nozzle and focusing lens assembly is incremented in the positive Z-direction, thereby building a three dimensional component layer additively.

It is important to control the thermal behavior to reproducibly fabricate parts. The ultimate intent is to monitor the thermal signatures and to incorporate sensors and feedback algorithms to control part fabrication. With appropriate control, the geometric properties (accuracy, surface finish, low warpage) as well as the materials' properties (e.g. strength, ductility) of a component can be dialed into the part through the fabrication parameters. Thermal monitoring techniques will be described, and their particular benefits highlighted. Preliminary details in correlating thermal behavior with processing results will be discussed.

Case Study with H13 Tool Steel
I. Thermocouple Measurements

A relatively easy way to obtain a thermal signature during processing is by inserting thermocouples directly into the sample during fabrication. Hollow, one line width wide shell boxes were fabricated from H13 tool steel with varying laser powers and traverse velocities (see Table I). Fine diameter (10 μm) Type C thermocouple wire was used for the measurements to ensure no reaction during deposition.


Table I. Parameters of fabrication for H13 tool steel shell box.

Parameter	Value
Material	H13 tool steel
Layer Thickness	0.125 mm
Traverse Velocity	6.0 and 9.3 mm/s
Power	200 and 300 W
X, Y Dimension	62.5 mm

Figure 1 shows the in-situ temperature readings from a representative thermocouple inserted during fabrication of a shell box processed at 200W and 6 mm/s. Each peak represents the thermocouple response as the laser passes over the thermocouple, from initial insertion to subsequent layer depositions. The data acquisition time is 0.3 seconds, so each spike represents many individual measurements during fabrication[*]. After the initial peak in temperature, the heat is quickly conducted away in about 40 seconds to a nominal value of 150 °C. Typically, this would result in a solidification process producing a high hardness, martensitic microstructure. However, for LENS processing, each subsequent pass reheats the previous layers, such that even after seven layers, the part receives a thermal 'hit' of 800 °C, and after eleven subsequent layers the thermocouple still receives a thermal excursion of 600 °C. Even after forty two deposition layers, the thermocouple reads a maximum temperature of 300 °C. After each deposition pass, the part cools down to 150 °C, but the part has received an integrated reheat which can adversely affect the material's properties including residual stress and mechanical strength due to tempering or aging effects.
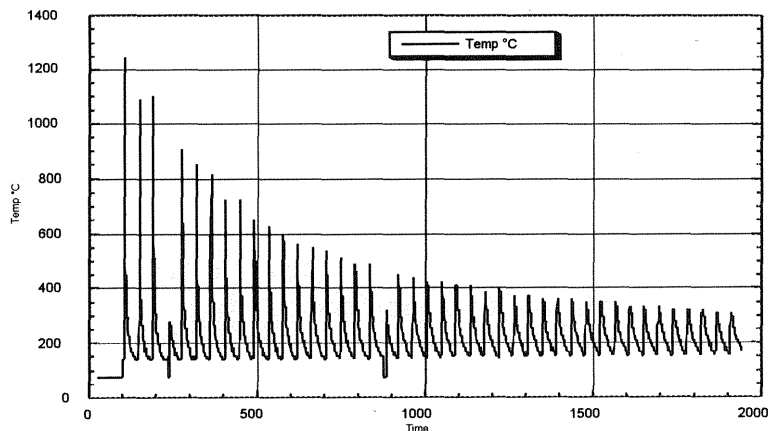
Figure 1. Thermocouple response (°C) versus time (seconds) during fabrication of H13 shell box.

II. Correlation between Thermal Behavior and Hardness for H13 Tool Steel

Figure 2 shows a cross-section of the top layers in the H13 hollow part processed at 200W with a 9.3 mm/s traverse velocity. The light area represents the last five layers of deposition (or approximately 870 μm), whereas the dark area represents the integrated temperature reheat or thermal cycling region. There is a definite change in microstructure between these two zones, as shown in Figure 3 with a dramatic decrease in hardness as the sample

---

[*] Absolute peak temperatures are higher than recorded because the thermocouple response time has not been incorporated.

is probed from the top region into the dark zone. The last five layers do not receive the integrated heat treatment and retain the martensitic phase with a high hardness value of 59 Rockwell C. The subsequent layers undergo many thermal excursions. Thermal cycles above 800 °C can re-austenize the material, and at 900 °C, this can happen in a matter of seconds. With many thermal cycles above 600 °C, it is possible to age or temper the material through reprecipitation or coarsening of the carbide distribution.

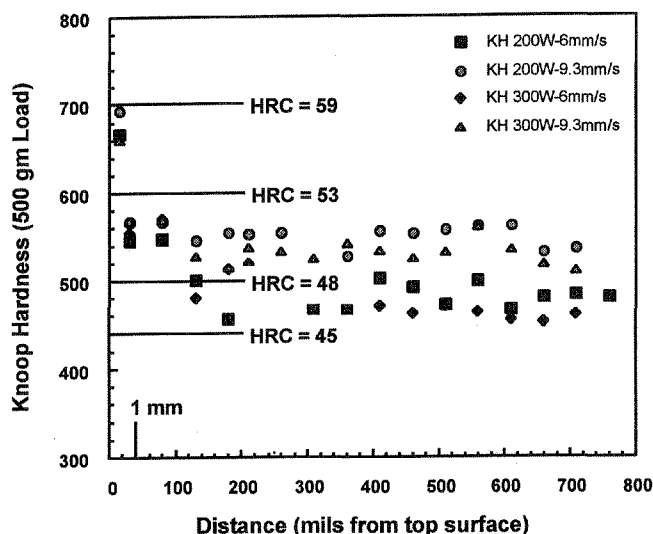Figure 2. Cross-section micrograph of H13 tool steel thin wall.

Figure 3. Hardness values (Knoop and Rockwell C, HRC) versus distance from top of wall for four processing conditions.

Even though these are preliminary results, these types of effects are evident from the microstructure shown in Figure 2. In the dark zone, the sample has experienced many thermal excursions above 600 °C, which corresponds to a reasonable amount of tempering or aging, where the expected hardness value, in the range of 50 Rockwell C (HRC)^2, is observed in our data (Fig 3). Fully understanding and controlling this transition is important for tailoring material properties.

In Figure 3, it is apparent that process parameters directly affect the properties, with traverse velocities having the greatest effect on the final hardness of the tool steel material. At a traverse velocity of 6 mm/s, the hardness ranges from 45 to 48 HRC; whereas at 9.3 mm/s, the hardness has a slightly higher value between 50 and 52 HRC. At increased speeds, the previous layers receive a shorter time excursion at the elevated temperatures producing reduced aging effects.

III. Residual Stress in H13 Tool Steel

Knowledge of the magnitude and distribution of residual stresses is often important because of their effect on structural behavior. A holographic-hole drilling technique[3] was used to determine the residual stress state in the shell samples. In the holographic-hole drilling method, a region of a test object containing stress is illuminated with laser light using an optical setup. A hologram of the region is made by exposing a recording plate in a commercially available holocamera to the light of a reference beam and that of the object beam as reflected from the test

object. The hologram is recorded electrostatically on an erasable, re-useable thermoplastic medium. Then a small square-bottomed hole is milled into the region of interest to a depth that can be varied, but which is generally a fraction of the hole diameter. The hole releases residual stresses locally, causing material surrounding the hole to deform in response to the stress relief. The resulting surface deformations, which are both in-plane and out-of-plane, alter the path length of the light reflected from the region, immediately creating a pattern of optical interference fringes on the hologram. The interference fringe pattern can then be analyzed to determine the residual stresses that existed prior to the introduction of the hole.
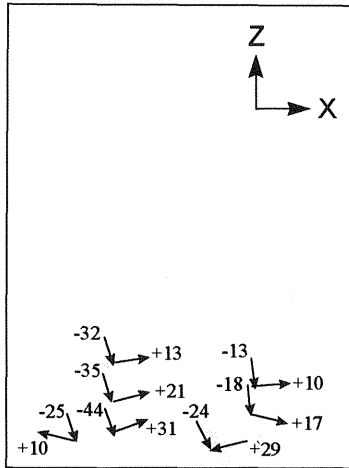
Figure 4. Principal residual stresses along H13 wall (magnitude and direction).
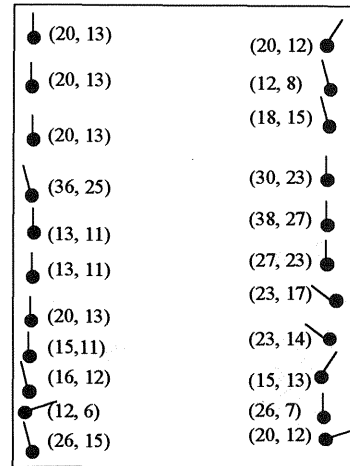
Figure 5. Principal residual stresses on surface of H13 solid part (depth=1mm).

Figure 4 shows the residual stress distribution along a wall processed at a laser power of 200W with a 6 mm/s traverse velocity. For these thin walled hollow shapes, the stress was only measured near the base of the sample to minimizing any distortions created during the drilling sequence. An unusual biaxial stress state was measured, where in the fabrication plane (X direction) the principal stress state is positive, or in tension, with values ranging from 10 to 31 ksi. However, in the through-layer condition (Z direction), the stress state is negative, or in compression, with values ranging from -13 to -44 ksi. It should be mention this material has a yield strength of 180 ksi, so the residual stress values are quite low with respect to the strength of the as-processed material (~20%). Further work is required to understand the biaxial stress state condition in these shell samples.

To clarify the effect of geometric influence on residual stress manifestation for H13 tool steel, a solid H13 tool steel sample was fabricated (6.4 cm x 1.0 cm x 11.4 cm). Figure 5 shows the distribution of principal stresses and their direction along one side measured in the as-processed material. The residual stress near the surface is in tension and has a low value ranging from 6-38 ksi, well below the yield strength of the material (180 ksi). In complex part fabrication, it is expected the overall residual stress state would be low for this alloy.

Initial evidence suggests that H13 solidification may occur as primary austenite or ferrite. If it occurs as ferrite, then it must undergo a transformation to austenite during cooling and this transformation would likely proceed in such a way as to reduce some of the stress. If

solidification occurs as primary austenite there would not be any stress relieving effect. However, at lower temperatures, the austenite (whether it is primary austenite or austenite formed from ferrite) transforms to martensite in this alloy (which has a high hardenability) rather than the diffusional decomposition products of ferrite and pearlite. This transformation to martensite is known to be affected by stress, and might act to reduce the stress (i.e. the dilatation that occurs during the transformation might reduce the residual stresses from differential thermal contractions). Moreover, each reheat cycle from subsequent deposition layers which heat the alloy back into the austenite phase field (say then next four or five layers based on the thermocouple data) will result in the formation of austenite. Here again, stresses which are present may tend to be relieved by the transformation dilatations. Finally, the tempering (alloy carbide precipitation) which occurs during reheats to peak temperatures below 900 °C also results in a dimensional change. It is conceivable that this tempering would also act in such a way that the dimension change would help to reduce the residual stresses.

Non-invasive Thermal Imaging Techniques

As discussed earlier, it is known intuitively that a thermal gradient exists across the molten pool and into the bulk material created by the LENS process. The nature and extent of this gradient has not been fully characterized. Since mechanical properties are dependent upon the microstructure of the material, which in turn is a function of the thermal history of solidification, an understanding of the temperature gradient induced by LENS processing is of special interest. It would be particularly beneficial to use non-invasive thermal imaging to measure the temperature profile and gradients and to use these thermal profiles in feedback control. Preliminary results for two techniques will be discussed: 1) infrared imaging for bulk temperature measurements plus gradients, and 2) high speed visible imaging to measure the molten pool temperature and its corresponding gradients. With these two techniques, it is possible to obtain a complete picture of the thermal behavior, near and far from the molten pool, during LENS processing. Initial experiments were conducted using stainless steel 316 powders.

I. Temperature Measurement Using Digital IR Imaging

In-situ temperature measurements were performed during LENS processing using a digital infrared camera, (Flir Systems, Prism DS). The camera's recording element is a 320 x 244 pixel platinum silicide CCD array, with a spectral range from 3.6 to 5 mm. The system records the infrared radiation emitted by a heated object, and, using various filters, may record the emission from objects with temperatures ranging from -10 °C to 1700 °C. Absolute temperature measurements require knowledge of the emissivity of the object. Since no emissivity values for metal objects fabricated using laser deposition are known, only relative temperature measurements have been performed. A discussion of a procedure for performing absolute temperature measurements, without knowledge of the object's emissivity will be discussed.

Figure 6 shows a thermal image taken with the digital camera. The laser is incident from the top of the frame, and the part is rastered from left to right to form a thin, one line width wide wall in stainless steel 316. The image shows the laser weld pool and the heat conduction into the surrounding metal.
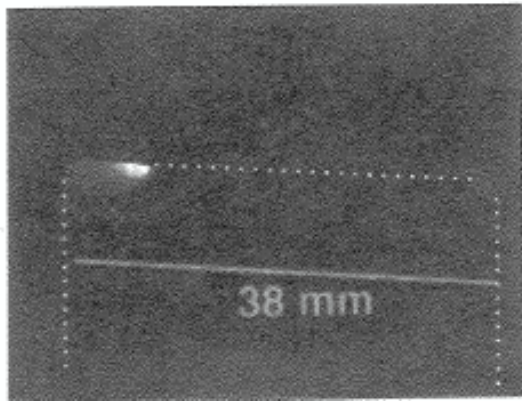
Figure 6. In-situ thermal image of LENS process for stainless steel 316 alloy.
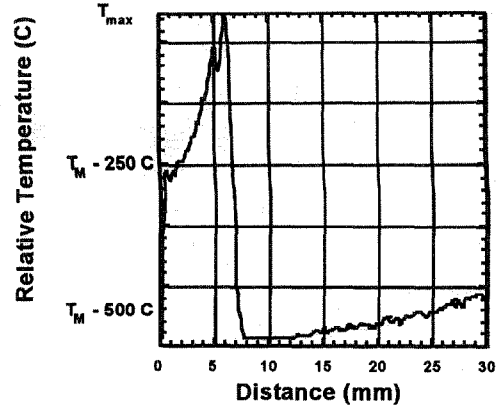

Figure 7. In-situ thermal profile of wall along the direction of travel (Fig. 6).

Figure 7 shows the thermal profile of Fig. 6 taken along to the direction of travel. Since the quantitative temperature is not known at this time, the relative temperature T_{max} is plotted as the maximum temperature measured by the IR camera near the weld pool region. The rest of the temperatures plotted are the values below this maximum temperature. The trace shows a steep profile in the region surrounding the molten pool (~36 K/mm), a cooler region to the right with a thermal signature that is not detectable, and another detectable heated region at the right corner of the part where the laser had completed the previous layer four second ago. The effect of the thermal profile on the previous layers is not shown in this figure. Figure 6 shows a large thermal tail as well a large thermal region of conduction into the previously deposited layers. With more analysis, a complete thermal picture will be developed for processing stainless steel 316 alloy.

In order to develop a procedure for determining absolute temperature using an infrared imager without knowledge of the object's emissivity, it is necessary to consider Planck's radiation law. The monochromatic energy density radiated by a blackbody is given by the Planck relation,

$$W(\lambda) = \frac{c_1 \lambda^{-5}}{e^{-c_2/\lambda T} - 1} \qquad [1]$$

where c_1 and c_2 are constants, l is the wavelength, and T is the temperature of the object[4]. An approximation to equation [1] is given by Wien's law,

$$W(\lambda) = c_1 \lambda^{-5} e^{-c_2/\lambda T} . \qquad [2]$$

The signal recorded by a detector element in the camera's focal plane is

$$S_i = \int_{\lambda_1}^{\lambda_2} \varepsilon W(\lambda) R(\lambda) d\lambda \qquad [3]$$

where ε is the emissivity of the object and $R(\lambda)$ is the detector response. As a further approximation,

$$S_i = \varepsilon c_1 \lambda_e (T)^{-5} e^{-c_2/\lambda T} R(\lambda) \qquad [4]$$

where $\lambda_e(T)$ is the temperature dependent effective wavelength. If an independent measurement of temperature is made at T_o, then the temperature T recorded by the ith detector element is related to the signal $S_{i,o}$ by

$$\frac{1}{T} = \frac{1}{T_0} + \frac{\lambda_e(T)}{c_2} \ln \frac{S_i}{S_{i,0}}$$

[5]

where $S_{i,o}$ is the signal recorded by the ith detector from an object at temperature T_o. Therefore, with a valid expression for $\lambda_e(T)$, the ratio of the signal at an unknown temperature to that at a known temperature may be used to obtain absolute temperature measurements without knowledge of the emissivity of the object. The set of experiments to calibrate the infrared camera is currently underway.

II. Temperature Measurement Using High Speed Visible Imaging

Preliminary experiments were conducted using ultra high speed digital imaging techniques[5] during LENS processing to provide insight as to the size of the molten pool and the thermal gradient in 316 stainless steel (SS316) samples fabricated using the LENS process. Digital images were obtained directly through a CaFl viewport in the LENS glovebox using a 12 bit digital camera equipped with a telephoto lens and 650nm broad band filter. A total of 2048 frames/run were recorded at a rate of 1.4 ms/frame. Temperatures were obtained using standard pyrometric techniques. The results shown are for SS316 material built using coarse powder (-150/+325 mesh) at a nominal laser power of 260W. A single, one line width wide wall was fabricated with 250 micron layer increments, where the traverse direction is from left to right.
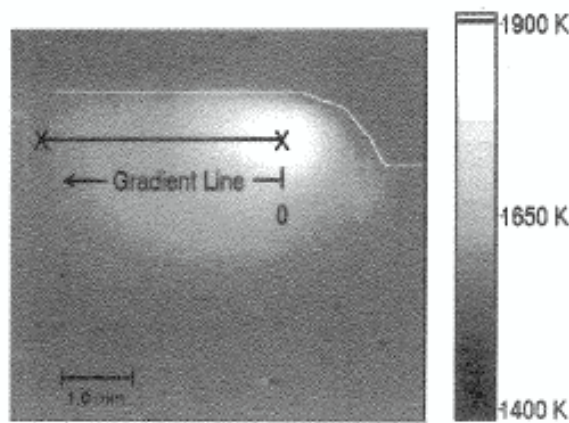
Figure 8. Digital image of molten pool and bulk material during LENS processing of SS316.

Figure 8 is a digital image of the molten pool and the adjacent bulk material created during processing. The field of view encompasses approximately 5 mm. A white line has been superimposed on the image to indicate material boundaries (i.e.; the top layer is being deposited on the previous layer with a curved profile in the region of the molten pool).

95

The temperature profile shown in Figure 9 and thermal gradient shown in Figure 10 correspond to the gradient line indicated in the digital image. Figure 9 shows that the molten pool reaches temperatures on the order of 1875 K (reasonably large superheat) with a linear decrease in temperature until thermal arrest (solidification) occurs at approximately 1650 K. Upon solidification, bulk material continues to cool similar to the thermocouple measurements. In Figure 10, the gradient at the center of the molten pool is zero, where immediately adjacent (~0.25 mm), the gradient is 150 K/mm. A maximum gradient of 160 K/mm is indicated in the region approximately 1 mm from the molten pool. The gradient decreases sharply with distance from the molten pool until solidification occurs, at which point the gradient levels out to approximately 20–30 K/mm. This agrees with the infrared data which measured approximately 36 K/mm near but not within the melt region of the molten pool.
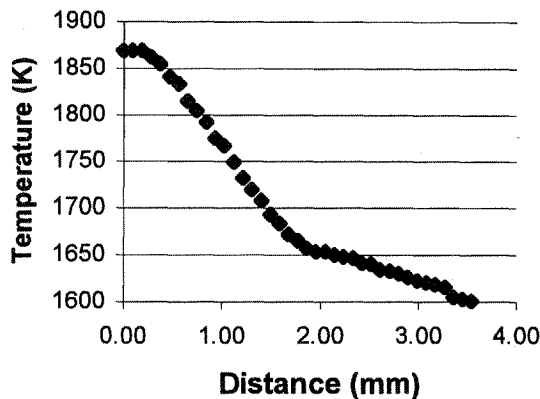

Figure 9. Temperature profile across
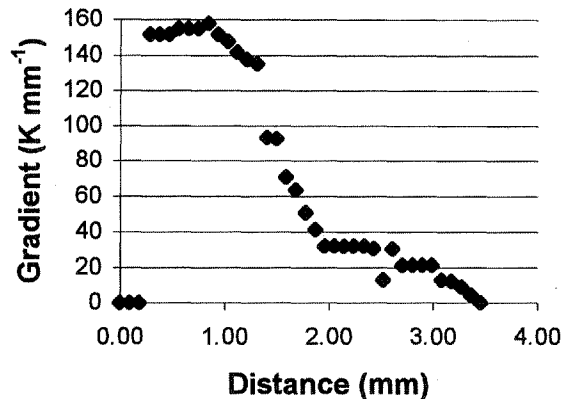gradient line indicated in Fig 8.

Figure 10. Thermal gradient across
gradient line indicated in Fig 8.

Summary

Knowledge of the thermal behavior is critical to reliable and repeatable fabrication during LENS processing. Our initial thermal experiments show promise in both monitoring as well as understanding the thermal behavior. With in-situ, calibrated real time monitoring, it will be possible to use these thermal signals for feedback control. Preliminary results show there is a significant effect on the microstructural evolution during fabrication of hollow H13 tool steel parts, where the integrated temperature reheat tempers the material.

References

[1] M. L. Griffith et. al., *Free Form Fabrication of Metallic Components using Laser Engineered Net Shaping (LENS)*, Proceedings of the Solid Freeform Fabrication Symposium, August 12-14, 1996, Austin, TX.
[2] G. Roberts, G. Krauss, R. Kennedy, Editors, Tool Steels, Fifth Ed., ASM International, Chapter 13, 1998.
[3] A. Makino and D. V. Nelson, E. A Fuchs, D. R. Williams, *Determination of Biaxial Residual Stresses by Holographic-Hole Drilling Technique*, J. of Engineering Materials and Technology, Vol. 118, 1996, p.583.
[4] M. R. Wehr. *Physics of the Atom*. Addison-Wesley:Reading, 1984, p.82.
[5] W.H. Hofmeister, R.J. Bayuzick, M.B. Robinson, *Noncontact Temperature Measurement of a Falling Drop*, International Journal of Thermophysics, Vol. 10, No. 1, 279 - 292.